An experimental study on water surface profiles of high Froude number flows

Park, Jae Hyeon; Park, Yong Sung; Kim, Young Do; Chae, Dong Seok

Published in:
KSCE Journal of Civil Engineering

DOI:
10.1007/s12205-017-0703-x

Publication date:
2018

Document Version
Peer reviewed version

An Experimental Study on Water Surface Profiles of High Froude Number Flows

Jae Hyeon Park[1], Yong Sung Park[2], Young Do Kim[3*], Dong Seok Chae[1]

[1]Dept. of Civil Engrg., Inje Univ., 197 Inje-ro, Gimhae, Gyeongnam, 50834, South Korea.

[2]Div. of Civil Engrg., Univ. of Dundee, Perth Rd., Dundee DD5 3LE, UK.

[3]Dept. of Environ. Engrg.(Nakdong River Environmental Research Center), Inje Univ., 197 Inje-ro, Gimhae, Gyeongnam, 50834, South Korea.

[*]Corresponding author, email: ydkim@inje.ac.kr

Abstract

Motivated by need to study supercritical overbank flows on floodplain, we experimentally investigate if initially supercritical flow in a rectangular flume would maintain its state throughout. Varying upstream gate opening, flow rate and angle of the slope, a total of 37 experimental cases were carried out. The experimental results are compared to two existing theories: an inviscid theory based on nonlinear shallow water equations and jump conditions and a hydraulic theory that takes friction into account. The experimental data are consistent with the two theories. Flows on downward slope were stable, while those on upward slope had unstable hydraulic jump and transformed into

subcritical flow. The reported results should serve well in designing a laboratory flume with the supercritical inflow and in conducting hydraulic model experiments on overbank flows.

Keywords: Froude number, hydraulic jump, water surface profile

1. Introduction

Overbank flows on a flood plain of a river with the streamwise velocity typically of order 1 m s^{-1} or faster and the depth of order 10 cm often become supercritical. Hydraulic model experiments, e.g. for riverbank revetment blocks, on such flows thus require supercritical flow as the upstream boundary condition. The stability of water surface profiles of such high-Froude number flows within a recirculating flume with a rectangular cross-section is of our concern in the present paper. In particular, we consider a situation in which the prismatic cross-section extends to the end of flume and the flow simply falls down the downstream end. In this specific configuration, the questions to be addressed are (i) if and when there is going to be a hydraulic jump and (ii) if the hydraulic jump will remain stable, in order to setup a guideline to avoid the hydraulic jump and the subsequent subcritical flow within the flume.

There are two relevant theoretical studies available in literature. One is an inviscid theory by Baines (1995) and Baines & Whitehead (2003) which is based on nonlinear shallow

47 water equations and jump conditions, and the other is a hydraulic theory of Defina &
48 Susin (2003) and Defina et al. (2008) in which bottom friction is taken into account.
49 According to the inviscid theory (Baines & Whitehead 2003), a hydraulic jump formed
50 on an adverse slope is always unstable and any displacement from its stable position will
51 result in continual moving of the hydraulic jump in the same direction as that of the
52 displacement. However in the context of engineering design of spillways, it has been
53 observed that hydraulic jump on an adverse slope becomes stable and stationary if the
54 Froude number upstream of the jump is sufficiently high (see e.g. McCorquodale &
55 Mohamed 1994; Pagliara & Peruginelli 2000). Defina & Susin (2003) proposed a
56 hydraulic theory which shows that hydraulic jumps in upward sloping channel could be
57 stable if there is sufficiently large friction which is parameterized by Chezy coefficient
58 (see Chow 1959). Note that both theories predict that hydraulic jumps on a downward
59 slope are always stable.
60
61 In the present paper, we report a new set of experimental data and compare them with the
62 two aforementioned theories. While both Baines & Whitehead (2003) and Defina et al.
63 (2008) also present their own experimental data, respectively, ours are different in the
64 sense that the former was done in a relatively small-scale flume (1.2 m long and 0.052 m
65 wide) and that the latter has a geometric configuration in which the location of the
66 hydraulic jump was controlled by downstream sluice gate as well. The new data set are
67 expected to be useful in designing and operating a recirculating flume with high-Froude
68 number flows and provide benchmarking data for numerical models.
69

In the next section, we first briefly review both the inviscid theory and the hydraulic theory. Then in section 3, the experimental setup and the procedure are reported. Analysis of the data and comparison with the two kinds of theories are presented in section 4. Finally, concluding remarks and further studies are discussed in section 5.

2. Theoretical background

Let d_0 be the initial undisturbed water depth measured normal to the bottom of the rectangular channel, q the flow rate per unit width, θ the angle of the channel bed to the horizontal with upward slope to be positive, L the length of the channel from the upstream sluice gate to the downstream end, $h_m = L\tan\theta$ the elevation of the downstream end of the channel bed measured from the elevation of the channel bed at the upstream sluice gate, and g the gravitational acceleration.

Baines (1995) shows that there are multiple steady flow states which can be determined by the initial Froude number,

$$F_0 = \frac{q}{\sqrt{g d_0^3}}, \tag{1}$$

and the height ratio,

$$H_m = \frac{h_m}{d_0}. \tag{2}$$

The flow regimes are depicted in figure 1, in which equations for the curves are as follows:

$$H_m = 1 - \frac{3}{2}F_0^{2/3} + \frac{1}{2}F_0^2 \quad \text{for} \quad 0 \le F_0 \le 4.47, \tag{3}$$

$$H_m = \frac{1 + \left(1 + 8F_0^2\right)^{3/2}}{16F_0^2} - \frac{1}{4} - \frac{3}{2}F_0^{2/3} \quad \text{for} \quad F_0 \ge 1, \tag{4}$$

and

$$F_0 = \left(H_m - 1\right)\left(\frac{1 + H_m}{2H_m}\right)^{1/2} \quad \text{for} \quad H_m \ge 1. \tag{5}$$

Figure 1. Flow regimes for hydrostatic free surface flow on a sloped channel: solid line, equation (3); dashed line, equation (4); dotted line, equation (5). Region (a) is where super- (and sub-)critical flow remains to be super- (and sub-)critical flow; region (b) is where three different flow states, namely supercritical flow, partially blocked flow and unstable stationary hydraulic jump, are all possible; region (c) is where partially blocked flow occurs; and region (d) is for completely blocked flow (adapted from Baines 1995).

In figure 1, regime (a) is where super- (and sub-)critical flow remains to be super- (and sub-)critical flow; regime (b) is where three different flow states, namely supercritical flow, partially blocked flow and unstable stationary hydraulic jump, are all possible;

109 regime (c) is where partially blocked flow occurs; and regime (d) is for completely
110 blocked flow. Here, partially blocked flow is the situation where part of flow reflects
111 back to upstream direction while the rest of flow overflows the obstacle, and the
112 completely blocked flow has no overflow at all. Note that the equations (3-5) are valid for
113 $H_m \leq 0$. For stable hydraulic jump to be possible for $H_m < 0$, as implied in figure 1, the
114 bottom friction should be accounted for (see Baines and White 2003). We also note here
115 that negative H_m are not indeed a properly defined state variable unlike its positive
116 counterpart. Nevertheless we choose to use it so that all the experimental data can be
117 presented in the same graph and the two theories could be compared.
118
119 For initially supercritical flow in a rectangular channel, the flow will remain supercritical
120 if it belongs to regime (a), or will become subcritical all the way up to the upstream sluice
121 gate with submerged hydraulic jump just downstream of the gate if the flow is classified
122 as regime (c) or (d). Because the possible stationary hydraulic jump in regime (b) is
123 unstable to infinitesimal disturbance (Baines & Whitehead 2003), practically only two
124 states (either supercritical flow or subcritical flow with a submerged hydraulic jump) are
125 possible in regime (b).
126
127 On the other hand, Defina and his coworkers (Defina & Susin 2003; Defina et al. 2008)
128 maintained that the hydraulic jump in regime (b) of figure 1 could be stable if there is
129 enough friction. Denoting Chezy coefficient in the upstream of the jump as χ, the stability
130 criterion is
131

$$\frac{\chi^2 \tan\theta}{g} < \frac{\left(1+\sqrt{1+8F_0^2}\right)^3}{32F_0^2} \tag{6}$$

for hydraulically smooth bed, and

$$\frac{\chi^2 \tan\theta}{g} < 2F_0^2 \frac{1-\left[0.5\left(-1+\sqrt{1+8F_0^2}\right)\right]^{-7/3}}{-3+\sqrt{1+8F_0^2}} \tag{7}$$

for fully rough bed. Note that, strictly speaking, the Froude number in equations (6) and (7) is different from that of equation (1) by a factor of $1/\cos\theta$. In our experiments however, θ varies between -2° and 2° and the associated error is less than 0.06%, which is negligible compared to the uncertainty in determination of Chezy coefficient. Also notice that the right-hand sides of both (6) and (7) are increasing function for large Froude numbers and asymptotically approach $F_0/\sqrt{2}$. The stability criteria shown in equation (6) and (7) are, therefore, consistent with the previous experimental observations such as those of McCorquadale & Mohamed (1994) and Pagliara & Peruginelli (2000).

3. Experimental setup and procedure

We used the high-speed water flume at the Environmental Water Resources Laboratory in the Department of Environmental Science and Engineering at Inje University, South

153 Korea. The water flume is made of smooth acrylic sheets (20 mm thick) and supported by
154 protruded aluminum frame, measuring 6 m long, 0.3 m wide and 0.3 m deep. The slope
155 of the flume can be adjusted to any angle between -5^o and 5^o (see figure 2).
156

Figure 2. A schematic diagram of the high-speed water flume.

157
158 The water flow is supplied by a submerged water pump (power: 30 hp; maximum
159 capacity: 0.2 m^3 s^{-1}) through 5 hoses. Each hose is fitted with an adjustable valve and the
160 flow rate is controlled by adjusting opening of the valves. The feed water first enters into
161 the pressurizing chamber before flowing into the working section of the flume so that a
162 very high flow velocity (2.7 m s^{-1} in horizontal bed and 3.5 m s^{-1} with downward slope in
163 typical water depth of order 0.1 m) can be achieved. Between the pressurizing chamber
164 and the working section of the flume, there is a sluice gate. Opening of the gate can also
165 be adjusted so that the flow velocity as well as the flow depth can be further controlled.
166 The flow rate is measured by an ultrasonic flowmeter (Ulsoflow 309P) and it essentially
167 varies linearly with the number of open valves.
168
169 Experiments consist of water surface profile measurements for each combination of three
170 parameters, namely (i) upstream gate opening, d_0; (ii) flow rate per unit width, q; and (iii)
171 angle of the slope, θ. A total of 37 experimental cases were carried out within a parameter
172 space defined by $3 \le d_0 \le 10$cm, $0.05 \le q \le 1.14$m^2 s^{-1}, and $-2 \le \theta \le 2°$ within
173 the ranges of safe operation of the facility, and are summarized in table 1.
174

Table 1. Experimental cases. In the last column, sub/jump/super indicates if the water

surface profile is entirely subcritical, there is a stable hydraulic jump within the channel, or the water surface profile is entirely supercritical.

Water depth, which is denoted as η, was measured at 18 stations that are distributed over the 5-m-long channel using tape rulers glued to the glass sidewall. Even in practically steady flow, water surface continually fluctuates due to random high-frequency surface waves generated by turbulence, and we adapted the following procedure to ensure the accuracy of water depth measurement. For each measurement, three readings were taken, namely maximum, minimum, and nominal values, and the measurement was repeated three times by the same observer at different times. Only when the standard deviation of the three ensemble measurements of a nominal value is less than 1%, the ensemble mean was taken as the measurement. Otherwise, the above process was repeated until satisfactory. The results are summarized in table 2.

Table 2. Measured water surface profiles (cm). The first row is the distance from the upstream sluice gate.

Once $\eta(x)$ is obtained, where x is the streamwise coordinate with the origin at the upstream sluice gate, corresponding Froude numbers $F(x)$ were calculated. Based on the Froude numbers, we determined if the flow in channel is entirely subcritical, has a stable jump, or is entirely supercritical, which are listed in table 1. Results of the classifications were also visually inspected during the experiments and confirmed.

3. Experimental results and discussion

196

197 Figure 3 shows examples of measured water surface profiles as well as the calculated
198 Froude numbers for three different types of flows.

199

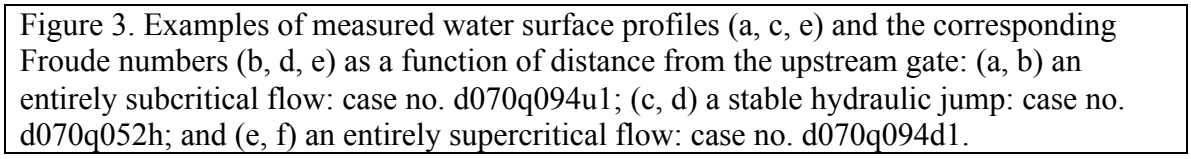

Figure 3. Examples of measured water surface profiles (a, c, e) and the corresponding Froude numbers (b, d, e) as a function of distance from the upstream gate: (a, b) an entirely subcritical flow: case no. d070q094u1; (c, d) a stable hydraulic jump: case no. d070q052h; and (e, f) an entirely supercritical flow: case no. d070q094d1.

200

201 It is interesting to note here that while the entirely supercritical flow maintains uniform
202 depth throughout the channel, the subcritical flow begins with much higher water depth
203 just downstream of the upstream sluice gate than the gate opening, then grows over the
204 submerged hydraulic jump, and decreases toward the critical flow at the downstream end.
205 Therefore one may conjecture that entirely subcritical flows would be classified as
206 regime (c) or (d) of figure 1, and that entirely supercritical flows as regime (a) of figure 1.

207

208 Flow regime of each experimental run is plotted in the parameter space of H_m and F_0 and
209 compared with the inviscid theory of equations (3) to (5) in figure 4.

210

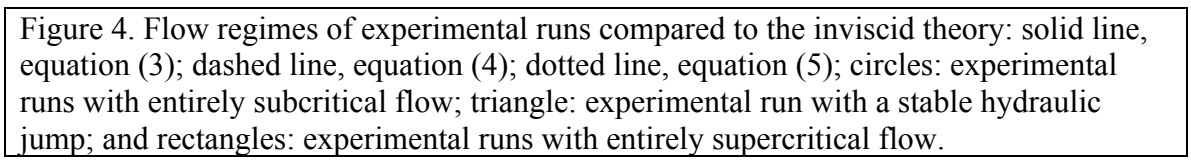

Figure 4. Flow regimes of experimental runs compared to the inviscid theory: solid line, equation (3); dashed line, equation (4); dotted line, equation (5); circles: experimental runs with entirely subcritical flow; triangle: experimental run with a stable hydraulic jump; and rectangles: experimental runs with entirely supercritical flow.

211

212 As expected, all the experimental cases with entirely subcritical flow fall in the regime
213 (c) of figure 1. There is one case (d070q052h) with a stable hydraulic jump on a
214 horizontal channel with its initial Froude number slightly less than one. The flow

contracts just downstream of the upstream gate and becomes supercritical before the jump occurs (see table 2). All the cases with downward slope and most cases in the horizontal channel are entirely supercritical and they are all classified as the regime (a) of figure 1.

On the other hand, there are three cases of entirely supercritical flow in adverse slope, in which two of them are in regime (c) and one is on the border between regimes (b) and (c). Those cases are d085q136u1, d070q136u1 and d030q052u1 in the order of increasing F_0. It is believed that those cases could have developed an unstable hydraulic jump and eventually become entirely subcritical flow, had the channel been much longer. Figure 5 shows water surface profiles and Froude numbers of the three cases.

Figure 5. Measured water surface profiles (a, c, e) and the corresponding Froude numbers (b, d, e) as a function of distance from the upstream gate for the three irregular cases in figure 4 (i.e. rectangles in regime c): (a, b) case no. d030q052u1; (c, d) case no. d070q136u1; and (e, f) case no. d085q136u1.

One can observe that the water surface elevation increases almost linearly throughout the length of the tank and the Froude number decreases accordingly for each of the three cases.

Another very interesting point in figure 4 is that flows seem to be possible for higher H_m than predicted by equation (5). We reiterate here that the nonlinear shallow water equation predicts that the equation (5) gives a minimum H_m for a given F_0, above which flow is completely blocked by the obstacle (the tip of the slope in the present case). We

suspect that undulation of the free surface spills over the end of the channel and makes flows possible for higher H_m, but further study is required to explain the discrepancy between the nonlinear shallow water theory and the experiment.

Now we turn our attention to the hydraulic theory. Before comparing out experimental data to the hydraulic theory, we first need to calculate the Chezy coefficient χ. For hydraulically smooth bed, χ may be given by (Chow 1959)

$$\frac{\chi}{\sqrt{g}} = 5.75 \log_{10}\left(a \frac{q\sqrt{g}}{\nu \quad \chi}\right), \tag{8}$$

in which a is an empirical constant and ν is kinematic viscosity. Defina et al. (2008) determined a to be 1.23 from their experiments, and we take a = 1 herein. Considering that a is within the logarithm, the result is safely insensitive to its value. Equation (8) was solved for each value of q using Newton-Raphson method and the result is summarized in table 1.

In figure 6, we compare our experimental results to the hydraulic theory. Note that a hydraulic jump, if ever happens, is supposed to be stable if it is located below the solid line in figure 6.

Figure 6. Flow regimes of experimental runs compared to the hydraulic theory: solid line, equation (6); circles: experimental runs with entirely subcritical flow; triangle: experimental run with a stable hydraulic jump; and rectangles: experimental runs with entirely supercritical flow. Note that a hydraulic jump, if ever happens, is supposed to be

stable if it is located below the solid line in the parameter space.

All the experiments with either horizontal or down-sloping channel are in the stable regime. In other words, had the channel been longer, there would have been a hydraulic jump in the channel and it would have stayed in that location. On the other hand, all the cases done in adverse slope are in the unstable regime. Most of the cases are entirely subcritical, except the three cases. Those cases coincide with those discussed earlier in relation to the inviscid theory (d085q136u1, d070q136u1 and d030q052u1). Once again the linearly increasing water surface profiles shown in figure 5 suggest that those cases could have been entirely subcritical with much longer channel length.

Overall both inviscid and hydraulic theories give similar predictions in our specific circumstances. It is because that the stability of the hydraulic jump largely depends on the slope of the channel. Difference between the two theories could only be felt if the bottom friction becomes drastically increased, for example, by increasing surface roughness. In our case, this may be achieved by decreasing the Chezy coefficient by at least a factor of 2 (or equivalently increasing Manning's n value by the same factor). Therefore, for experimental facility fitted with smooth bottom, both inviscid and hydraulic theories would provide the same result regarding the stability of hydraulic jumps.

4. Concluding remarks

Hydraulic experiments on overbank flows on flood plain often require supercritical flow

as the upstream boundary condition, and the stability of the water surface profile is of interest in such cases. We have carried out experiments in a recirculating flume of rectangular cross-section varying three parameters, namely the upstream gate opening, flowrate and angle of the slope. The results were compared to the two kinds of existing theories: an inviscid theory and a hydraulic theory, and the experimental data were consistent with the both theories. In fact, as long as the stability of the hydraulic jump in a channel fitted with smooth bottom is concerned, either theory can be used as the criterion.

Acknowledgements

This research was supported by a grant (12-TI-C02) from Construction Technology Innovation Program funded by Ministry of Land, Infrastructure and Transport of Korean government (MLIT, KAIA). YSP also acknowledges the financial support from the Royal Society of Edinburgh/Scottish Government Personal Research Fellowship Co-Funded by the Marie-Curie Actions.

References

Baines, P. G. *Topographic Effects in Stratified Flows*. (1995). Cambridge University Press, Cambridge.

Baines, P. G. & Whitehead, J. A. (2003). On multiple states in single-layer flows. *Phys.*

Fluids, **15**, 298-307.

Chow, V. T. (1959). *Open Channel Hydraulics*. McGraw Hill, New York.

Defina, A. & Susin, F. M. (2003). Stability of a stationary hydraulic jump in an upward sloping channel. *Phys. Fluids*, **15**, 3883-3885.

Defina, A., Susin, F. M. & Viero, D. P. (2008). Bed friction effects on the stability of a stationary hydraulic jump in a rectangular upward sloping channel. *Phys. Fluids*, **20**, 036601.

McCorquadale, J. A. & Mohamed, M. S. (1994). Hydraulic jumps on adverse slopes. *J. Hydraul. Res.,* **32**, 119-130.

Pagliara, S. & Peruginelli, A. (2000). Limiting and sill-controlled adverse-slope hydraulic jump. J. Hydraul. Engng, 126, 847-851.

Table 1. Experimental cases. In the last column, sub/jump/super indicates if the water surface profile is entirely subcritical, there is a stable hydraulic jump within the channel, or the water surface profile is entirely supercritical.

	d_0 (m)	q ($m^2 s^{-1}$)	θ (°)	F_0	H_m	χ	sub/jump/super
d030q052u2	0.030	0.052	2	3.22	5.82	61.67	sub
d030q052u1	0.030	0.052	1	3.22	2.91	61.67	super
d030q052h	0.030	0.052	0	3.22	0.00	61.67	super
d030q052d1	0.030	0.052	-1	3.22	-2.91	61.67	super
d030q052d2	0.030	0.052	-2	3.22	-5.82	61.67	super
d050q052u2	0.050	0.052	2	1.49	3.49	61.67	sub
d050q083u2	0.050	0.083	2	2.36	3.49	64.86	sub
d050q052u1	0.050	0.052	1	1.49	1.75	61.67	sub
d050q095h	0.050	0.095	0	2.70	0.00	65.80	super
d050q052d1	0.050	0.052	-1	1.49	-1.75	61.67	super
d050q095d1	0.050	0.095	-1	2.70	-1.75	65.80	super
d050q095d2	0.050	0.095	-2	2.70	-3.49	65.80	super
d070q052u2	0.070	0.052	2	0.90	2.49	61.67	sub
d070q095u2	0.070	0.095	2	1.63	2.49	65.80	sub
d070q052u1	0.070	0.052	1	0.90	1.25	61.67	sub
d070q094u1	0.070	0.094	1	1.63	1.25	65.78	sub
d070q136u1	0.070	0.136	1	2.34	1.25	68.34	super
d070q052h	0.070	0.052	0	0.90	0.00	61.67	jump
d070q094h	0.070	0.094	0	1.63	0.00	65.78	super
d070q136h	0.070	0.136	0	2.34	0.00	68.34	super
d070q095d1	0.070	0.095	-1	1.63	-1.25	65.80	super
d070q136d1	0.070	0.136	-1	2.34	-1.25	68.34	super
d070q136d2	0.070	0.136	-2	2.34	-2.49	68.34	super
d085q052u2	0.085	0.052	2	0.67	2.05	61.67	sub
d085q095u2	0.085	0.095	2	1.22	2.05	65.80	sub
d085q052u1	0.085	0.052	1	0.67	1.03	61.67	sub
d085q095u1	0.085	0.095	1	1.22	1.03	65.80	sub
d085q136u1	0.085	0.136	1	1.75	1.03	68.34	super
d085q136h	0.085	0.136	0	1.75	0.00	68.34	super
d085q095d1	0.085	0.095	-1	1.22	-1.03	65.80	super
d085q136d1	0.085	0.136	-1	1.75	-1.03	68.34	super
d085q136d2	0.085	0.136	-2	1.75	-2.05	68.34	super
d100q052u2	0.100	0.052	2	0.53	1.75	61.67	sub
d100q095u2	0.100	0.095	2	0.96	1.75	65.80	sub
d100q052u1	0.100	0.052	1	0.53	0.87	61.67	sub
d100q095u1	0.100	0.095	1	0.96	0.87	65.80	sub
d100q136u1	0.100	0.136	1	1.37	0.87	68.34	super

Table 2. Measured water surface profiles (cm). The first row is the distance from the upstream sluice gate.

x	0.0	15.0	30.0	60.0	90.0	120	150	180	210	240	270	300	330	360	390	420	450	480
d030q052u2	19.2	17.3	17.3	19.8	21.8	21.2	20.6	19.3	17.9	17.3	15.9	14.9	13.8	12.7	11.7	10.5	9.0	7.0
d030q052u1	2.4	2.0	1.8	2.0	2.7	2.2	2.4	2.7	2.9	3.1	3.2	3.1	3.8	3.5	3.8	3.9	4.3	4.4
d030q052h	2.4	1.9	2.2	2.1	2.4	2.3	2.6	2.4	2.6	2.8	3.2	2.8	3.4	3.4	3.1	3.5	3.1	3.4
d030q052d1	2.5	2.0	2.1	2.2	2.4	2.4	2.3	2.3	2.3	2.7	2.9	2.8	2.9	3.1	2.8	2.7	3.0	2.9
d030q052d2	2.3	1.8	2.0	2.2	2.4	2.2	2.2	2.2	2.1	2.7	2.8	2.7	2.5	3.0	2.8	2.3	2.5	2.8
d050q052u2	22.3	21.1	21.1	21.6	22.4	21.6	20.8	19.2	18.3	17.2	16.1	15.0	13.6	12.5	11.7	10.4	8.9	6.9
d050q083u2	21.1	18.9	19.4	22.8	25.5	24.8	24.0	22.9	21.9	21.2	19.2	17.6	17.0	15.6	14.4	13.0	11.2	8.6
d050q052u1	11.4	11.3	14.0	15.2	15.8	15.0	14.6	14.1	13.2	12.7	11.7	11.2	10.7	10.1	9.6	9.0	8.1	6.5
d050q095h	3.5	2.6	2.2	3.2	3.8	3.8	3.8	3.6	3.7	3.9	4.1	4.5	4.2	4.3	4.3	4.5	4.2	4.6
d050q052d1	2.0	2.7	4.0	3.1	3.0	4.3	3.0	3.1	4.2	3.6	3.3	4.0	3.2	3.5	4.0	3.1	4.1	3.8
d050q095d1	3.6	2.6	2.7	3.3	3.7	3.7	3.8	3.5	3.5	3.6	5.1	4.5	4.4	4.5	4.7	4.7	5.3	5.4
d050q095d2	3.9	2.6	2.7	3.3	3.7	3.7	3.8	3.5	3.5	3.6	5.1	4.5	4.4	4.5	4.7	4.7	5.3	5.4
d070q052u2	23.3	22.8	22.2	22.9	23.0	21.8	21.2	19.6	18.6	17.3	15.9	15.0	13.9	12.8	11.7	10.4	9.2	6.9
d070q095u2	23.5	22.3	22.5	24.8	26.1	25.9	25.0	23.7	22.2	21.2	19.7	18.7	17.5	16.3	15.3	13.9	12.1	9.6
d070q052u1	15.0	14.9	15.8	16.7	16.6	15.7	15.4	14.6	13.9	13.1	12.0	11.6	11.0	10.6	9.9	9.0	8.1	6.5
d070q094u1	11.9	11.6	16.5	19.0	21.1	20.4	19.2	19.5	17.8	17.1	15.9	15.2	14.6	14.1	13.5	12.6	11.8	9.4
d070q136u1	5.9	4.2	4.0	4.8	3.7	5.0	5.2	5.0	5.4	5.7	6.2	5.9	5.6	6.5	6.4	6.2	6.2	6.6
d070q052h	5.7	4.6	4.4	4.7	4.9	4.8	4.8	6.0	7.8	7.8	6.8	6.1	5.8	5.7	6.0	6.7	6.3	6.0
d070q094h	5.1	4.1	4.4	4.4	4.7	4.6	4.6	4.9	5.4	5.7	5.7	5.7	5.4	5.9	6.2	5.5	5.7	6.0
d070q136h	5.8	4.6	4.7	4.4	4.6	4.6	5.3	5.2	5.3	5.9	6.1	5.4	5.4	5.1	5.9	6.0	5.5	5.7
d070q095d1	5.8	4.8	5.0	4.4	4.8	4.5	4.5	4.5	4.9	5.1	5.0	5.1	4.4	4.6	4.9	5.2	5.1	4.4
d070q136d1	5.7	4.3	3.7	3.6	4.2	4.2	4.7	4.9	4.6	5.0	5.3	5.4	5.0	4.7	5.0	5.3	5.5	5.1
d070q136d2	5.8	4.4	4.3	4.6	3.9	4.8	4.7	4.9	4.8	4.9	5.2	5.0	4.7	4.4	4.6	5.0	5.1	4.9

Table 2. (continued)

x	0.0	15.0	30.0	60.0	90.0	120	150	180	210	240	270	300	330	360	390	420	450	480
d085q052u2	22.7	21.9	21.7	22.1	21.8	20.9	19.9	19.1	17.7	16.7	15.5	14.5	13.6	12.6	11.7	10.5	9.1	7.0
d085q095u2	23.2	21.7	22.4	25.0	25.5	24.9	24.2	22.9	22.2	20.6	19.5	18.4	17.4	16.4	15.3	13.6	12.4	9.4
d085q052u1	15.5	15.5	16.1	16.8	16.3	15.7	15.1	14.5	13.9	13.3	12.5	11.8	11.4	10.6	9.9	9.3	8.5	6.7
d085q095u1	14.6	15.4	17.7	20.0	20.7	19.7	19.4	18.7	17.9	17.6	16.3	15.3	14.8	14.3	13.7	12.7	11.5	9.1
d085q136u1	7.1	5.4	4.7	4.6	5.0	6.1	6.0	6.0	6.3	6.6	6.6	7.0	6.7	7.0	7.5	7.3	7.8	7.7
d085q136h	6.9	4.7	5.1	4.7	5.4	6.0	6.0	5.8	6.2	6.6	6.5	6.7	6.5	6.4	6.6	6.9	7.1	6.6
d085q095d1	7.3	5.9	6.0	5.3	5.6	5.9	5.6	5.6	5.6	5.6	6.5	5.8	5.1	6.0	5.8	6.0	5.9	5.7
d085q136d1	7.1	5.3	4.6	4.8	4.9	5.4	5.2	5.2	5.8	6.0	6.3	5.8	5.6	5.8	5.7	6.1	6.1	6.2
d085q136d2	6.7	5.2	5.3	4.9	5.1	5.8	5.2	5.4	5.3	5.2	6.1	5.4	5.5	5.3	5.7	5.4	5.3	5.2
d100q052u2	23.6	22.6	22.6	22.2	21.6	20.5	19.5	18.4	17.2	16.1	14.9	13.9	12.9	12.0	11.0	9.8	8.5	6.3
d100q095u2	24.9	24.5	23.8	24.6	25.0	24.2	23.4	22.0	20.9	19.7	19.0	17.5	16.5	15.5	14.3	13.0	11.4	8.8
d100q052u1	15.7	15.5	16.3	16.0	15.7	14.9	14.4	13.8	12.9	12.4	11.5	10.9	10.4	10.0	9.4	8.5	7.8	6.4
d100q095u1	16.6	16.7	18.4	19.2	19.3	18.7	18.0	17.3	16.7	15.9	15.1	14.5	13.9	13.4	12.6	11.7	10.7	8.5
d100q136u1	15.1	15.9	18.9	21.9	22.5	21.6	21.3	20.4	19.7	18.9	17.9	17.2	16.6	16.0	15.4	14.4	13.2	10.4

Figure 1. Flow regimes for hydrostatic free surface flow on a sloped channel: solid line, equation (3); dashed line, equation (4); dotted line, equation (5). Region (a) is where super- (and sub-)critical flow remains to be super- (and sub-)critical flow; region (b) is where three different flow states, namely supercritical flow, partially blocked flow and unstable stationary hydraulic jump, are all possible; region (c) is where partially blocked flow occurs; and region (d) is for completely blocked flow (adapted from Baines 1995).

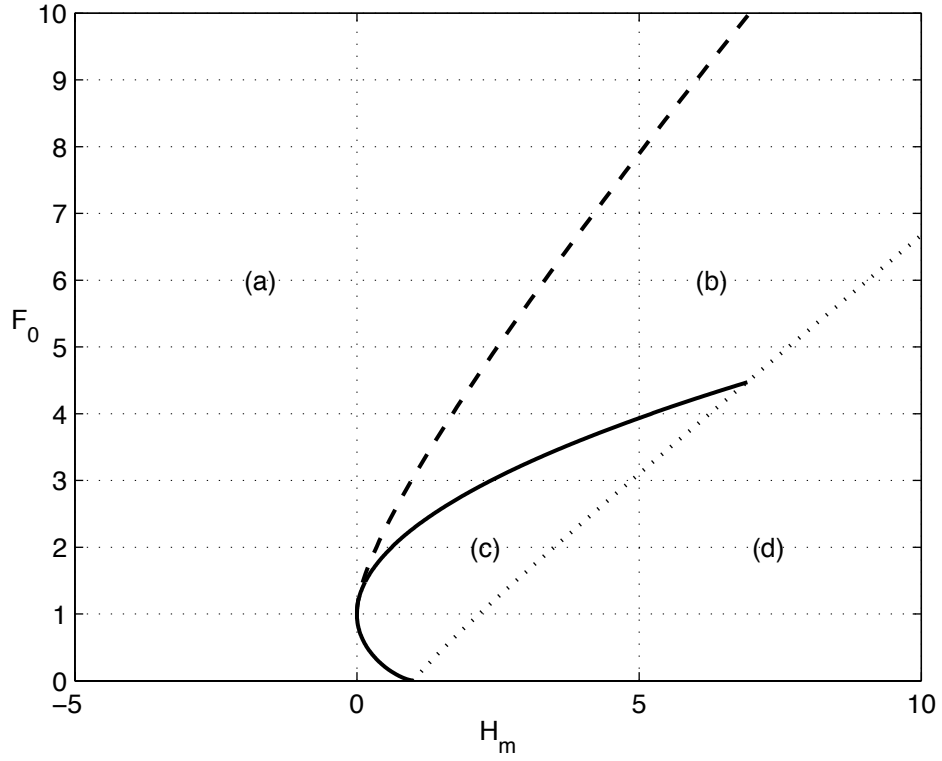

Figure 2. A schematic diagram of the high-speed water flume.

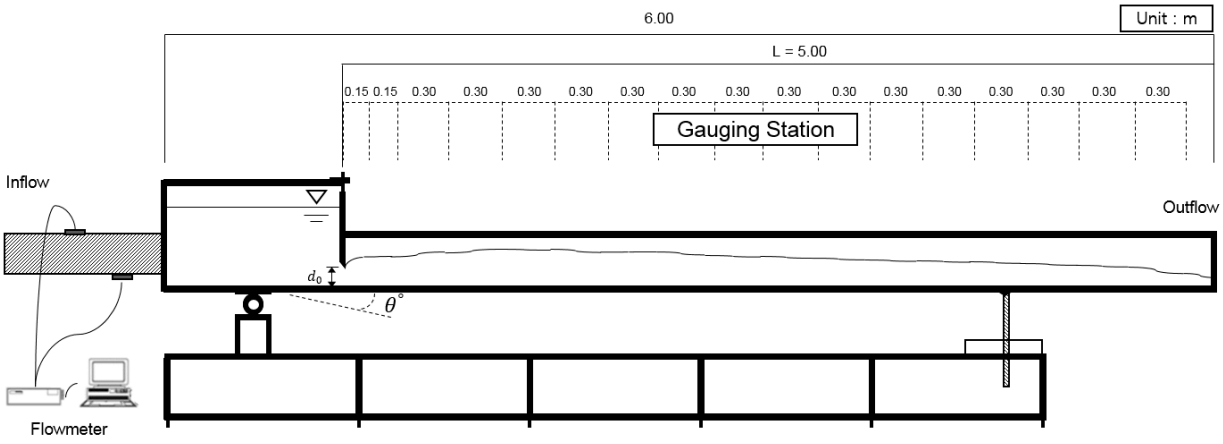

Figure 3. Examples of measured water surface profiles (a, c, e) and the corresponding Froude numbers (b, d, e) as a function of distance from the upstream gate: (a, b) an entirely subcritical flow: case no. d070q094u1; (c, d) a stable hydraulic jump: case no. d070q052h; and (e, f) an entirely supercritical flow: case no. d070q095d1.

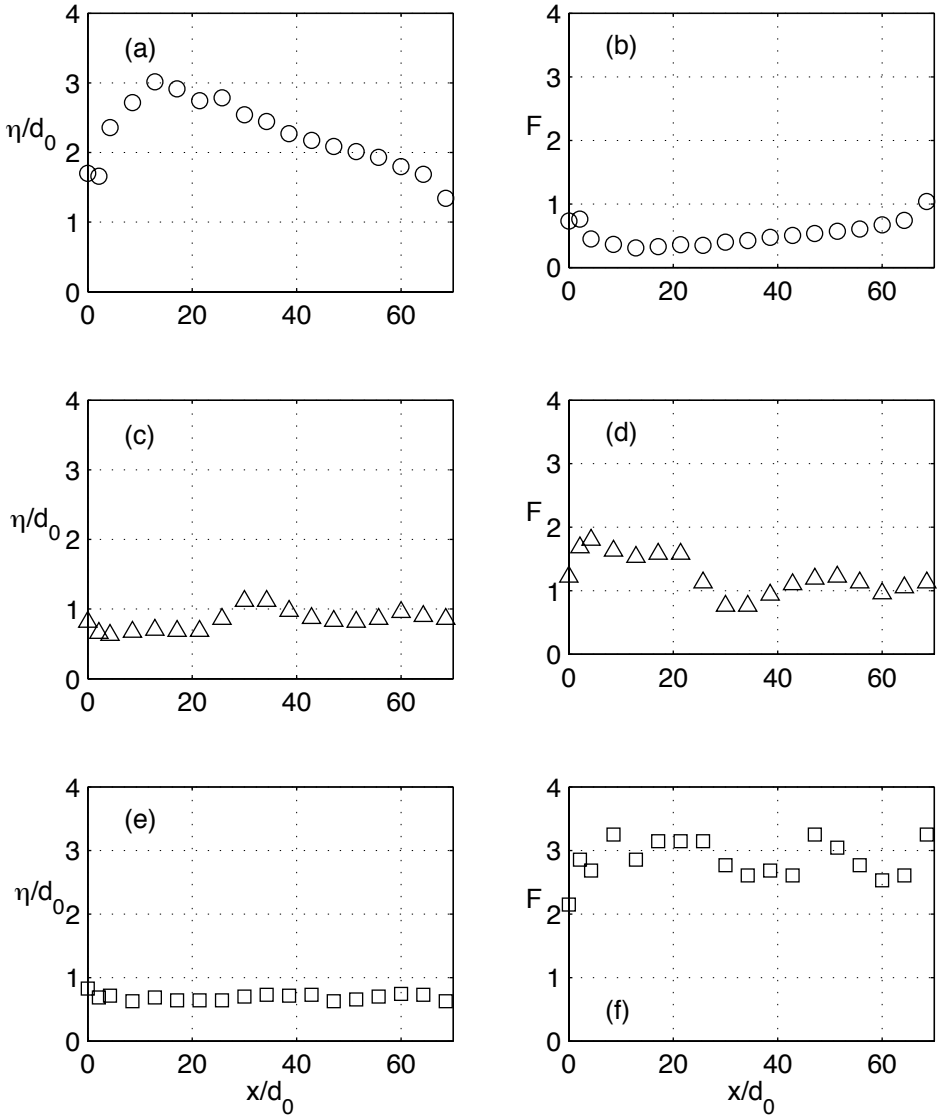

Figure 4. Flow regimes of experimental runs compared to the inviscid theory: solid line, equation (3); dashed line, equation (4); dotted line, equation (5); circles: experimental runs with entirely subcritical flow; triangle: experimental run with a stable hydraulic jump; and rectangles: experimental runs with entirely supercritical flow.

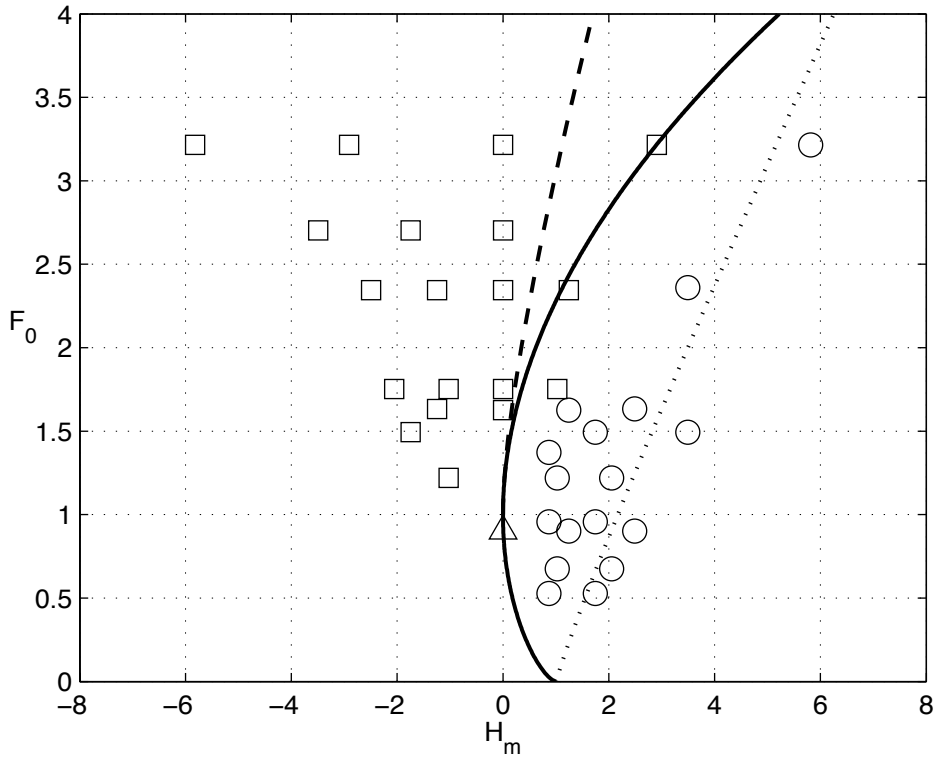

Figure 5. Measured water surface profiles (a, c, e) and the corresponding Froude numbers (b, d, e) as a function of distance from the upstream gate for the three irregular cases in figure 4 (i.e. rectangles in regime c): (a, b) case no. d030q052u1; (c, d) case no. d070q136u1; and (e, f) case no. d085q136u1.

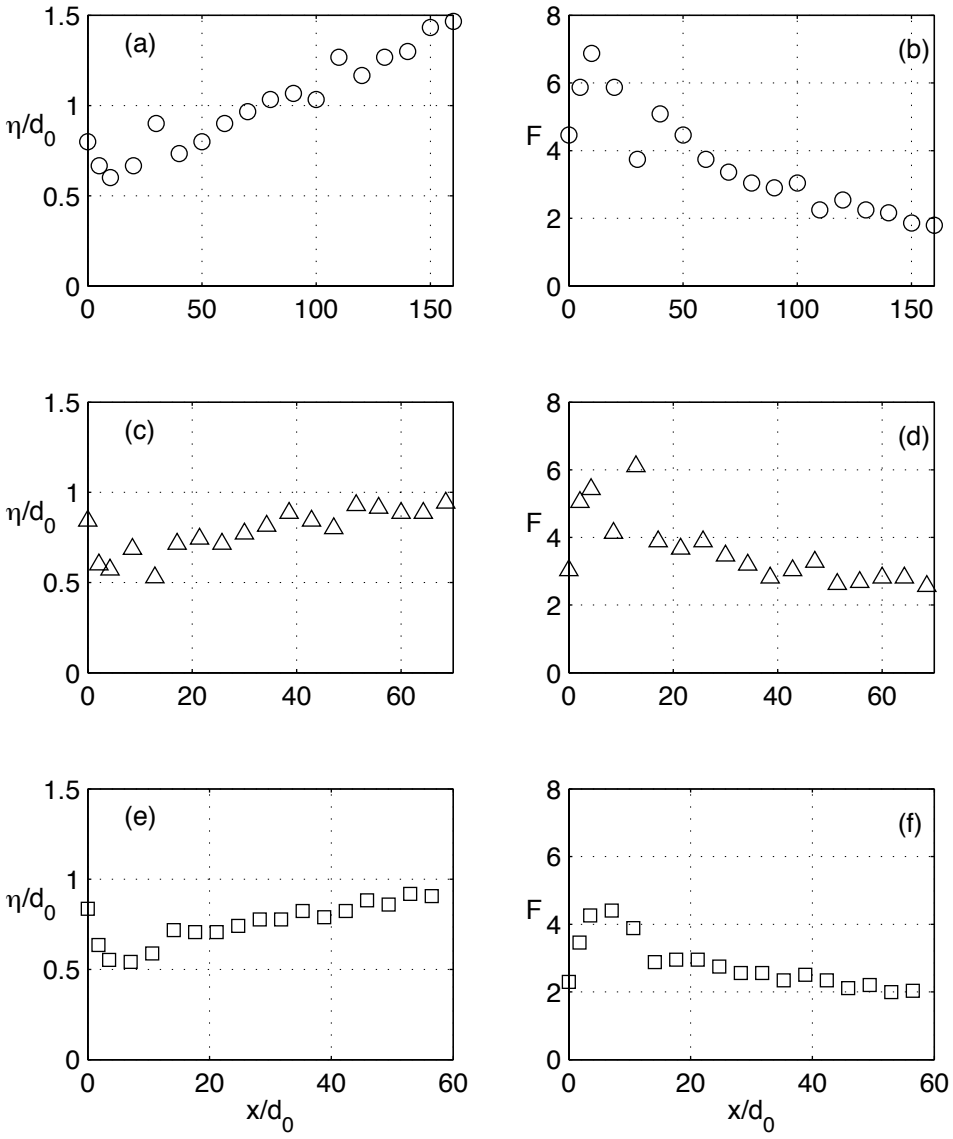

Figure 6. Flow regimes of experimental runs compared to the hydraulic theory: solid line, equation (6); circles: experimental runs with entirely subcritical flow; triangle: experimental run with a stable hydraulic jump; and rectangles: experimental runs with entirely supercritical flow. Note that a hydraulic jump, if ever happens, is supposed to be stable if it is located below the solid line in the parameter space.